INTERNATIONAL JOURNAL OF PRECISION ENGINEERING AND MANUFACTURING Vol. 14, No. 12, pp. 2149-2155 DECEMBER 2013 / 2149
DOI: 10.1007/s12541-013-0291-8

Increasing the Output from Piezoelectric Energy Harvester Using Width-Split Method with Verification

Chow Man Sang[1], Jedol Dayou[1,#] and Willey Y. H. Liew[2]

1 Energy, Vibration and Sound Research Group (e-VIBS), School of Science and Technology, Universiti Malaysia Sabah, Jalan UMS, Kota Kinabalu, Sabah, Malaysia, 88400
2 School of Engineering and Information Technology, Universiti Malaysia Sabah, Jalan UMS, Kota Kinabalu, Sabah, Malaysia, 88400
Corresponding Author / E-mail: jed@ums.edu.my, TEL: +60-88-320-000, FAX: +60-88-435-324

KEYWORDS: Piezoelectric energy harvester, Ambient vibration, Wideband operation, Quality factor, Structural damping, Energy conversion

This paper proposes a new scheme for piezoelectric energy harvesting maximization. The proposed enhancement relies on a new topology of splitting a specified dimension piezo composite bender into beams with smaller width and, therefore, higher quality factor (or Q factor). The increase of Q factor allows a much more effective energy conversion process. It is shown that the proposed method, based on single splitting, increases the harvested power by a factor of up to √6, and up to √7.62 for two even-splitting compared to with no splitting. The wideband operation is accomplished by using different resonating benders in such a way that individual benders are each tuned to a different resonance frequency. Taking the configuration of single even-splitting as an example, the power output of the prototype was 39 μW at 27.2 Hz with 8 Hz bandwidth under 2 mm peak-to-peak input displacement and 3 Hz variation in resonant frequency. This corresponds to more than 2 times of power output with no splitting as well as about 23% increase in bandwidth. Such power output is sufficient to power up electronics devices such as a "2 AA dry cells-powered" digital clock with the wider range operating frequency.

Manuscript received: April 15, 2013 / Accepted: October 19, 2013

1. Introduction

Energy from surroundings can be renewed with suitable choice of energy harvesting systems. For example, photovoltaic cells are used to harvest electricity from sunlight, the pyroelectric materials convert heat into electric energy, and the piezoelectric materials are particularly good for renewing the wasteful ambient vibration into useful electricity. Due to its low output power density, many researchers have proposed different methods to optimize the harvested energy from piezoelectric materials. Tien and Goo[1] demonstrated the use of piezo composite generating element (PCGE), in energy harvesting applications and evaluated its electricity generating performance. Karami et al.[2] used different piezoelectric materials, substrates, and configurations to identify the best design configuration for lightweight energy harvesting devices for low-power applications. Knight et al.[3] optimized the interdigitated (d_{33}) piezoelectric MEMS unimorph cantilever beams for harvesting vibration energy and tuning resonators by considering the effects of electrode patterns and dimensions on the real piezoelectric material poling. In another work on optimization of power output by Baker et al. was carried out using a tapered beam.[4] A complete review of current state of piezoelectric energy harvester based on vibration has been discussed in detail in reference.[5]

Kauffman and Lesieutre[6] developed a mathematic algorithm to describe the behaviour of a unimorph or bimorph annular-shaped piezoelectric vibration energy harvester. Roundy and Wright[7] developed a model for a piezoelectric energy harvester, and used their derived expression to predict the power output. Ottman et al.[8] explored the effect of impedance matching of the piezoelectric generator to the external load through the use of a DC-DC converter. The circuit was designed to dynamically optimize the power flow from the piezoelectric device. Lefeuvre et al.[9] introduced the synchronized charge extraction technique with inductor to improve the conversion efficiency of the bridge-type rectifying circuit. Some researchers had been actively searching for new form of materials for the purpose of energy harvesting.[10,11] In the past, the study of the piezoelectric harvesting systems focused on the physical properties of the piezoelectric material, the configurations of the piezoelectric transducer and power conditioning circuits. From the review of the literature, no one had reported work on investigating the method of reducing damping on the energy harvesting process. In this paper, the effect of the width-splitting for a fixed dimension piezoelectric material was modeled theoretically and investigated experimentally to increase the harvested power over a

wider range of excitation frequencies. This research work contributes to the present optimization studies of the piezoelectric energy harvesting with advantages of keeping the lowest costs, not much modifying the natural frequency and even direct use without conditioning circuit for some applications.

2. Theory of Operation

A piezo composite bender consists of a layer of piezoelectric PVDF film and a layer of host of similar dimensions bonded together. External stress acting on the PVDF film due to base vibration causes deflection to the bender. The deflection distorts the internal dipole moments within the PVDF film and this generates charges on the PVDF film. From reference,[12] the piezoelectric constitutive equations can be expressed in matrix form as

$$\begin{bmatrix}\varepsilon_1\\ \varepsilon_2\\ \varepsilon_3\\ \varepsilon_4\\ \varepsilon_5\\ \varepsilon_6\\ E_1\\ E_2\\ E_3\end{bmatrix}=\begin{bmatrix} s^D_{11} & s^D_{12} & s^D_{13} & 0 & 0 & 0 & 0 & 0 & g_{31}\\ s^D_{12} & s^D_{11} & s^D_{13} & 0 & 0 & 0 & 0 & 0 & g_{31}\\ s^D_{13} & s^D_{13} & s^D_{33} & 0 & 0 & 0 & 0 & 0 & g_{33}\\ 0 & 0 & 0 & s^D_{44} & 0 & 0 & 0 & g_{15} & 0\\ 0 & 0 & 0 & 0 & s^D_{44} & 0 & g_{15} & 0 & 0\\ 0 & 0 & 0 & 0 & 0 & s(s^D_{11}-s^D_{22}) & 0 & 0 & 0\\ 0 & 0 & 0 & 0 & g_{15} & 0 & \beta^\sigma_{11} & 0 & 0\\ 0 & 0 & 0 & g_{15} & 0 & 0 & 0 & \beta^\sigma_{22} & 0\\ -g_{31} & -g_{31} & -g_{33} & 0 & 0 & 0 & 0 & 0 & \beta^\sigma_{33}\end{bmatrix}\begin{bmatrix}\sigma_1\\ \sigma_2\\ \sigma_3\\ \sigma_4\\ \sigma_5\\ \sigma_6\\ D_1\\ D_2\\ D_3\end{bmatrix} \quad (1)$$

where E is the electric field strength, D is the electric charge displacement, σ is the mechanical stress, ε is the strain, β^σ is the reciprocals of permeability at constant stress, and s^D is the elastic compliances at constant electric charge displacement. The first subscript number of the g constants refers to direction of the supplied electric field and the second number refers the direction of material deformation.

Consequently, the piezo bender under the influence of external vibration experiences stress along the x (horizontal) direction is given by[13-15]

$$\sigma_{piezo} = Y_{piezo}(\varepsilon_{piezo} - g_{31}D_3) \quad (2)$$

where ε_{piezo}, g_{31} and D_3 are the strain on the piezo, the piezo stress constant and the electrical displacement along the z direction, respectively.

The electric charge harvested by the piezo film due to an external force, F, can be obtained by integrating the electric displacement to its overlapping area.[13-16] Therefore, the harvesting of electric charge for the film can be expressed as:

$$Q_0 = \int_0^{w_0}\int_0^{L} D_3 dy dx = \frac{-3AB(1-A+AB)g_{31}\varepsilon_r\varepsilon_0 L^2 F}{t_{bender}{}^2 k} \quad (3)$$

where

$$A = \frac{t_{host}}{t_{bender}} \quad (4)$$

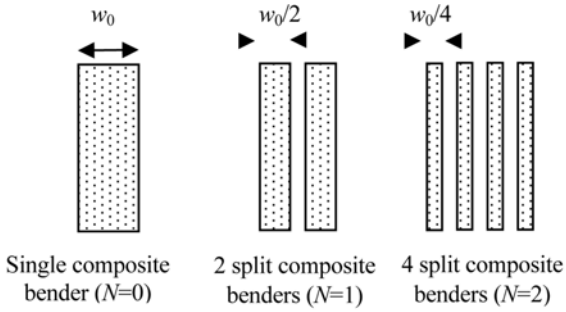

Fig. 1 Composite bender(s) with no splitting, in single even splitting and in two even splitting, respectively

$$B = \frac{Y_{host}}{Y_{piezo}} \quad (5)$$

$$k = h(1-A+AB)(1+Y_{piezo}g_{31}{}^2\varepsilon_r\varepsilon_0) - 39(1-A)(A)^2(B)^2 Y_{piezo}g_{31}{}^2\varepsilon_0 \quad (6)$$

and

$$h = 1+(A)^4(1-B)^2 - 2A(2(A)^2-3A+2)(1-B) \quad (7)$$

ε_0 and ε_r are the permittivity of the vacuum and the relative permittivity of the material, respectively, t_{host} is the host thickness, t_{bender} is the piezo composite bender thickness, Y_{host} is the Young's Modulus of the host, Y_{piezo} is the Young's Modulus of the film, L and w_0 are the length and width of the piezo bender, respectively.

The open circuit voltage of the piezo bender in Laplace Transform can be expressed in form of[13-16]

$$V_N(s) = I(s)Z_p(s) = sQ(s)\left(\frac{1}{sC_N}\right) \quad (8)$$

where Z_p and C_N are piezo impedance and piezo capacitance benders in parallel with N even splitting, respectively.

In this paper, the piezo composite bender used consists of a thin piezoelectric PVDF film adhering to a polypropylene substrate as a host of similar dimensions. This bender is folded and then split equally. Figure 1 illustrates the composite bender used before splitting (i.e., N=0), single even-splitting (N=1) of the bender into 2 split benders, two even-splitting (N=2) of the bender into 4 split benders. w_0 is the width of the initial single composite bender.

The piezo composite bender can be modeled mechanically as a single degree of freedom system (SDOF), which consists of an equivalent spring constant K of the piezo composite bender, an equivalent mass M, a dashpot with damping coefficient c, and a vibrating base. The equivalent SDOF model is shown in Fig. 2, where $d(t)$ is the vibrating base displacement and $x(t)$ is the equivalent mass displacement. $y(t)$ is the relative motion between the vibrating base and the equivalent mass, M.

The dynamic model of the piezo bender is expressed as[16]

$$\frac{V_N(s)}{\ddot{d}(s)} = \left(\frac{-3AB2^N(1-A+AB)g_{31}\varepsilon_r\varepsilon_0 L^2 K}{t_{bender}{}^2 k C_N}\right)\frac{1}{s^2+\frac{2\pi f_0 s}{Q_N}+(2\pi f_0)^2} \quad (9)$$

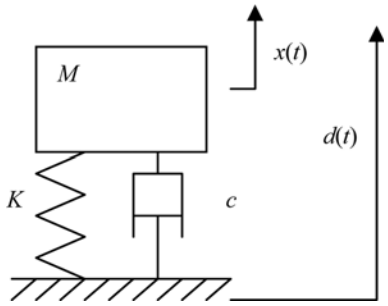

Fig. 2 Equivalent SDOF model for the piezo composite bender with excitation at base

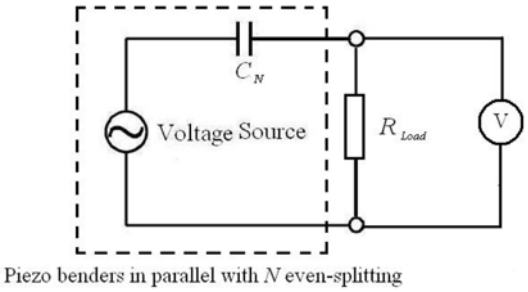

Fig. 3 The piezoelectric circuit model connected with a load resistor, R_{Load}

When a sinusoidal input $d(t)=d_o\sin(2\pi ft)$ is applied to the base excitation, the peak piezoelectric voltage generated with mechanical-electrical model can be obtained as[16]

$$V_N=\left(\frac{-3AB(2^N)(1-A+AB)g_{31}\varepsilon_r\varepsilon_0L^2K}{{t_{bender}}^2kC_N}\right)\sqrt{\frac{r^2+Q_N^2}{r^2+[Q_N(1-r^2)]^2}} \quad (10)$$

where

$$Q_N=\frac{f_0}{\Delta f} \quad (11)$$

is the quality factor or simply Q factor. f_0 is the natural frequency, Δf is the $3dB$ bandwidth of the N-th number of even splitting of initial piezo bender and $r=f/f_0$ is the ratio of the vibrating frequency to the natural frequency.

When an external resistive load is added to the output of the piezocomposite benders in parallel with N even splitting as shown in Fig. 3, the root mean square (rms) voltage across the resistive load can be obtained from potential divider of the circuit as shown in Fig. 3[14]

$$V_{Load,N,rms}=\Psi\sqrt{\frac{r^2+Q_N^2}{(R_{Load}^2+(2\pi fC_N)^{-2})(r^2+[Q_N(1-r^2)]^2)}} \quad (12)$$

where

$$\Psi=\left(\frac{-3AB(2^N)(1-A+AB)g_{31}\varepsilon_r\varepsilon_0L^2Kd_0R_{Load}}{\sqrt{2}{t_{bender}}^2kC_N}\right) \quad (13)$$

The average power output in the resistive load is obtained as

$$P=\frac{{V_{Load,N,rms}}^2}{R_{Load}} \quad (14)$$

The natural frequency of the piezo composite bender can be determined using

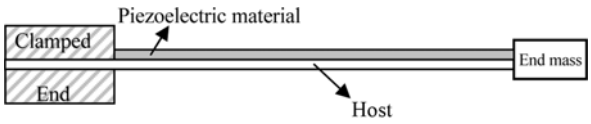

Fig. 4 Changing natural frequency of the piezo composite bender with end mass

$$f_o=\frac{1}{2\pi}\sqrt{\frac{K}{M}} \quad (15)$$

The equivalent mass, M, of the bender with end mass attached at free end is given by

$$M=\frac{33}{140}M_{bender}+M_{end} \quad (16)$$

where M_{bender} and M_{end} are the masses of the piezo composite bender and the end mass, respectively.

Sobocinski et al.[17] have proposed to vary the length of each beam to change the bandwidth of the harvesting system. Since their work focuses only on the wideband operation, the power density harvested reduces because they use a large and heavy non-resonant benders for widening the bandwidth. In order to secure the high output power as well as wide bandwidth of the specific size of the initial piezo composite bender discussed in this paper, the natural frequency for each reduced-width benders needs to be altered so that they are all having different natural frequencies before they are connected in parallel. In this study, the dimensions of the piezo composite bender are not varied. Referring to Eq. (15) and Eq. (16), noting that

$$f_0\propto\frac{1}{\sqrt{\frac{33}{140}M_{beam}+M_{end}}} \quad (17)$$

The alteration of the natural frequency of each of the reduced-width benders in this paper can be achieved by modifying the end mass attached to each bender as shown in Fig. 4.

3. Materials and Methods

In this paper, the bender is built using the piezoelectric PVDF film from Measurement Specialties, Inc. (MSI) (thickness is 52 μm and Young's modulus is 3×10^9 Nm^{-2}) and the substrate material of polypropylene (thickness is 124 μm and Young's modulus is 0.9×10^9 Nm^{-2}). The piezo stress constant, g_{31}, and the relative permittivity, ε_r, for the MSI piezoelectric film are given as 216×10^{-3} m^{2}C^{-1} and 13, respectively. The length and width of the single composite bender are 45 mm × 20 mm, respectively. The effective mass is 0.15 g. With this configuration, the single composite bender as well as each of its split benders has the same natural frequency, f_0, of 27.2 Hz. The benders with each even splitting is then set into harmonic vibration by a shaker with fixed input base displacement of 2.0 mm and range of vibrating frequencies (21~32 Hz) applied. The base displacement, d_0, is set as 2.0 mm. The resistive load used in the experiment is from 1 MΩ to 10 MΩ.

The experiment setup is shown in Fig. 5. The load voltage is measured

Fig. 5 Setup of the experiment with the single piezo composite bender

for each of the set vibration frequency. The load power at each vibration frequency can be calculated using Eq. (9). The experiment continues with splitting the initial piezo bender equally into two (N=1) and into four (N=2), separately, under the same setup and same experimental procedures. The variation of natural frequency of 1 Hz is chosen for the two reduced width benders with N=1 One bender remains its original natural frequency (i.e., 27.2 Hz) and another is adjusted to 26.2 Hz by modifying the end mass. For the four reduced width benders with N=2, one bender remains its original natural frequency of 27.2 Hz and other three benders are adjusted with equal interval to 26.9 Hz, 26.5 Hz and 26.2 Hz, respectively by modifying the end mass. The experiment continues with the variation of natural frequency of 3 Hz is chose two reduced width benders with N=1 (i.e., 27.2 Hz and 24.2 Hz) and four reduced width benders with N=2 (i.e., 27.2 Hz, 26.2 Hz, 25.2 Hz and 24.2 Hz), separately, under the same setup and same experimental procedures.

4. Results and Discussion

The load power for different load resistances can be seen in Fig. 6 at the damped resonant frequency for the piezo composite bender without splitting, in single even splitting and two even splitting, respectively. Observing Fig. 6, the optimum load power at the load resistance of 2 MΩ is noted for each of the three splitting configurations. This shows that the load resistance of 2 MΩ matches the internal impedance of the piezoelectric film for the maximum output power. It is also noted from Fig. 6 that the optimum power for the piezoelectric film in two even-splitting configurations is the highest and that without splitting is the lowest.

Figure 7 shows the simulations (Q=4.20, 5.15 and 6.33 for N=0, 1 and 2 respectively) and experimental results for the piezo bender without splitting, in single even splitting and two even splitting, respectively. The maximum load power for single even splitting has increased by a factor of 6 from that without splitting as well as the maximum load power for two even splitting has increased by a factor of 7.62 from that without splitting.

The damped natural frequencies of the piezo composite bender without splitting, in single even splitting and two even splitting can be determined from Fig. 7. They were identified to be 25.0 Hz, 26.6 Hz and 27.1 Hz, respectively. The resonance frequency of the bender in this case is dependent on its thickness and length. It is independent on its width. However, damping effect is dependent to surface area of the bender in vibrating. With the constant thickness and length of the

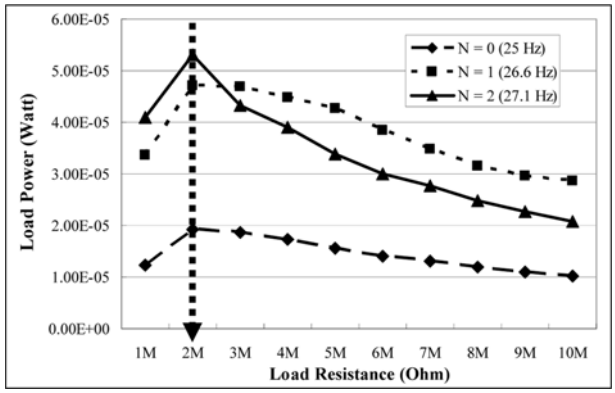

Fig. 6 Load power as a function of resistance for piezo composite bender at damped resonant frequency

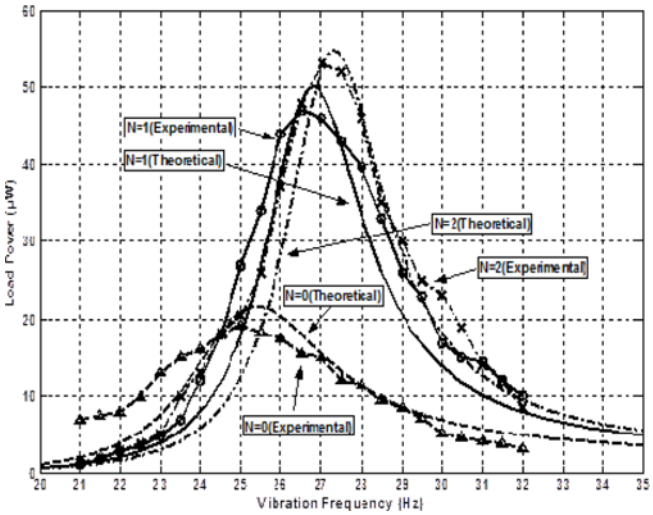

Fig. 7 Power-frequency response on external optimum resistive load of 2 MΩ

bender, the damping degree of the vibration decreases as the width of the bender decrease. Under the damped vibration, the largest vibrating amplitude, which results in highest power harvesting, occurs at the damped resonant frequency. From the damping theory, the damped resonance frequency is always lower than the undamped resonance frequency. It is understood that the variation between the damped resonance frequency and undamped resonance frequency decreases as the difference in damping decreases. From Fig. 7, it can be seen that the bender without splitting (0-fold) has larger surface area as compare to that of the bender in single even splitting (1-fold). Therefore, damped resonance frequency for the bender without splitting (0-fold) is much lower than the undamped resonance.

The output power generated increases as the number of fold increases. However, the rate of increment of the output power is expected to reduce as the power generated approaches a certain fraction of the input power. As for this work, the splitting is limited to 2-fold (N=2) due to limitation in available splitting instrument. There could be certain number of splits that beyond this will give no further significant increment in the power output. However, this is beyond the scope of the present work. The main focus of this work is to show that splitting the piezoelectric materials will increase the power output.

Table 1 Summary of experimental results. Δf is the bandwidth of the piezobenders in Heartz

Number of Fold, *N*/ width of each split PVDF film	Damped Natural Frequency	*Q* factor	Output power	Power factor increased compared to *N*=0	Δf (Hz)
N=0/ 20 *mm* (1)	25.0 *Hz*	4.20	19.2 μW		6.5
N=1/ 10 *mm* (2 benders)	26.6 *Hz*	5.15	47.0 μW	√6	5.3
N=1/ 10 *mm* (2 benders) with the variation of natural frequency of 1 Hz			44.0 μW	√5.25	5.8
N=1/ 10 *mm* (2 benders) with the variation of natural frequency of 3 Hz			39.0 μW	>2	8.0
N=2/ 5 *mm* (4 benders)	27.1 *Hz*	6.33	53.0 μW	√7.62	4.3
N=2/ 5 *mm* (4 benders) with the variation of natural frequency of 1 Hz			49.0 μW	√6.51	5.0
N=1/ 5 *mm* (4 benders) with the variation of natural frequency of 3 Hz			42.0 μW	√4.78	7.2

Figure 8 shows experimental results for the piezo composite benders in single even-splitting with no variation, variations of 1 Hz and 3 Hz from the resonant frequency, respectively. Similarly, Fig. 9 shows experimental results for the piezo composite benders in two even-splitting with no variation, variations of 1 Hz and 3 Hz from the resonant frequency, respectively.

Table 1 summarizes these significant findings (such as *Q* factor, load power, factor increase of the harvested power compared with *N*=0 and Δf) from the experiment. It can also be seen that the bandwidth increases with an increase in the variation of natural frequency. This is corresponds to a lower peak in the power responds of the harvester as shown in Fig. 8. However, there is still a gain in output power (for example, configuration with single even-splitting is more than 2 times of that without splitting for 3 Hz variation in resonant frequency). This shows that the maximum output power of the harvesting system is still ensured with wider bandwidth feature.

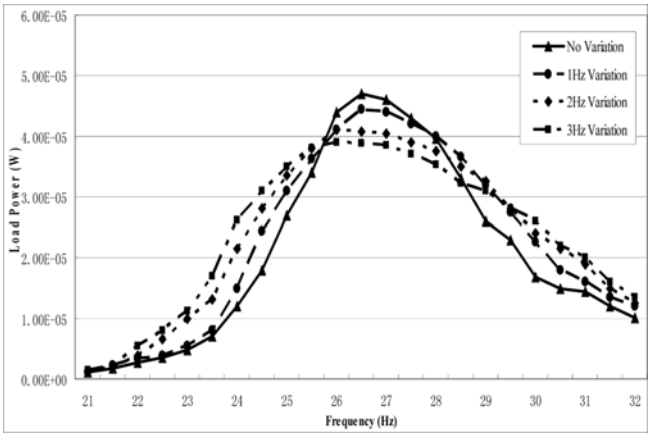

Fig. 8 Comparison of load power for piezo composite bender in single even-splitting with no variation in natural frequency, variations of 1 Hz and 3 Hz, respectively

5. Experimental Verification of the Optimized Piezoelectric Energy Harvesting System

The previous analysis shows that the proposed split-width method with wideband operation has the effect of increasing the energy conversion in the initial stage before the effective power conditioning circuit is added for further optimization. Other benefits with this method are simple in setup, wide bandwidth to harvest ambient vibration and direct use without conditioning circuit for certain applications. To verify this, an experiment was carried out to power-up a digital clock that requires a two AA size dry cell battery (1.5 volt each). There were two modes of piezoelectric harvester tested: the first mode is using a single PVDF piezoelectric film from Measurement Specialties, Inc. (MSI) with the thickness of 52 μm, and length and width of 45 mm × 20 mm, respectively; the second mode is using the same type of piezoelectric but with two split benders that is with reduced width of 10 mm.

The piezoelectric bender was excited at its base with displacement input of 2 mm. It can be seen that with the single piezoelectric harvester shown in Fig. 10(a), the digital clock was not in operating mode due to insufficient power input from the piezoelectric harvester. However, when the piezoelectric was split into two with identical dimensions, the digital clock was successfully turned into operating mode as shown in Fig. 10(b). This is understood that with the single split of the piezoelectric, the output power increased more than double even with the single split of the piezobender (refer to Table 1). It should be noted here that the same displacement input of 2 mm was used for both cases (for Figs. 10(a) and 10(b)) where they were excited at their respective resonance frequency.

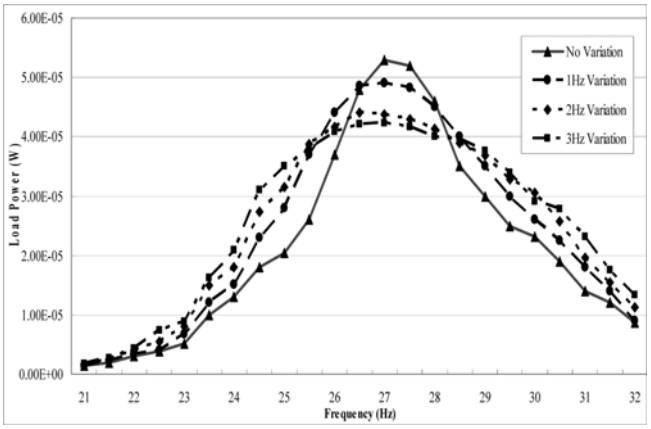

Fig. 9 Comparison of load power for piezo composite bender in two even-splitting with no variation in natural frequency, variations of 1 Hz and 3 Hz, respectively

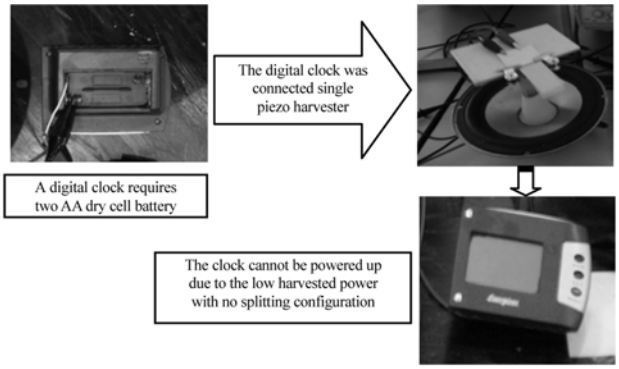

a. Using single piezoelectric bender with dimensions of 52 μm x 45 mm x 20 mm.

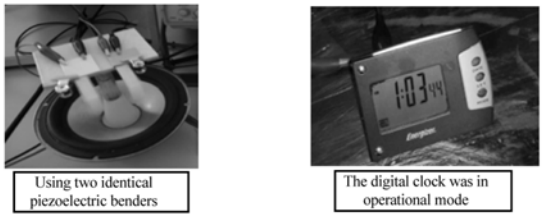

b. Using two identical piezoelectric bender with dimensions of 52 μm x 45 mm x 10 mm.

Fig. 10 Experimental verification of width-splitting piezoelectric harvester to power-up a 2AA battery digital clock. An input base excitation of 2 mm was used at their respective resonance frequency

6. Conclusion

The method of splitting the given piezoelectric material is proposed in this paper to maximize the current piezoelectric energy harvesting system. When the number of even-splitting increases, the width of each split piezo composite bender reduces and results in more effective energy conversion process and, therefore, a higher Q factor. The experimental result has shown that the harvested power was increased by a factor of up to 6 compared with no splitting and it increases the harvested power by a factor of up to 7.62 compared with no splitting based on two even-splitting. The wideband operation is accomplished by using different resonating benders in such a way that individual benders are each turned to a different resonance frequency. With 3 Hz variation in natural frequency to the split benders in single even-splitting as the example, the power output of the prototype was increased more than 2 times of power output with no splitting as well as about 23% increase in bandwidth. The application of the optimized piezoelectric energy harvester was successfully verified on a digital clock.

ACKNOWLEDGEMENT

This study was supported by the Malaysian Ministry of Science, Technology and Innovation (MOSTI) under Science Fund 03-01-10-SF0144, and is greatly acknowledged.

REFERENCES

1. Tien, C. M. T. and Goo, N. S., "Use of a Piezocomposite Generating Element in Energy Harvesting," Journal of Intelligent Material Systems and Structures, Vol. 21, No. 14, pp. 1427-1436, 2010.
2. Karami, M., Bilgen, O., Inman, D. J., and Friswell, M. I., "Experimental and Analytical Parametric Study of Single-crystal Unimorph Beams for Vibration Energy Harvesting," Ultrasonics, Ferroelectrics and Frequency Control, IEEE Transactions on, Vol. 58, No. 7, pp. 1508-1520, 2011.
3. Knight, R., Mo, C., and Clark, W., "MEMS Interdigitated Electrode Pattern Optimization for a Unimorph Piezoelectric Beam," Journal of Electroceramics, Vol. 26, No. 1-4, pp. 14-22, 2011..
4. Baker, J., Roundy, S., and Wright, P., "Alternative Geometries for Increasing Power Density in Vibration Energy Scavenging for Wireless Sensor Networks," Proc. of Alternative Geometries for Increasing Power Density in Vibration Energy Scavenging for Wireless Sensor Networks, pp. 959-970, 2005.
5. Kim, H., Kim, J.-H., and Kim, J., "A Review of Piezoelectric Energy Harvesting Based on Vibration," Int. J. Precis. Eng. Manuf., Vol. 12, No. 6, pp. 1129-1141, 2011.
6. Kauffman, J. L. and Lesieutre, G. A., "A Low-order Model for the Design of Piezoelectric Energy Harvesting Devices," Journal of Intelligent Material Systems and Structures, Vol. 20, No. 5, pp. 495-504, 2009.
7. Roundy, S. and Wright, P. K., "A Piezoelectric Vibration Based Generator for Wireless Electronics," Smart Materials and Structures, Vol. 13, No. 5, pp. 1131-1142, 2004.
8. Ottman, G. K., Hofmann, H. F., Bhatt, A. C., and Lesieutre, G. A., "Adaptive Piezoelectric Energy Harvesting Circuit for Wireless Remote Power Supply," Power Electronics, IEEE Transactions on, Vol. 17, No. 5, pp. 669-676, 2002.
9. Lefeuvre, E., Badel, A., Richard, C., Petit, L., and Guyomar, D., "A Comparison between Several Vibration-powered Piezoelectric Generators for Standalone Systems," Sensors and Actuators A: Physical, Vol. 126, No. 2, pp. 405-416, 2006.
10. Yun, S., Kim, J., and Lee, K. S., "Evaluation of Cellulose Electro-active Paper Made by Tape Casting and Zone Stretching Methods," Int. J. Precis. Eng. Manuf., Vol. 11, No. 6, pp. 987-990, 2010.
11. Kim, J., Lee, H., and Kim, H., "Beam Vibration Control Using Cellulose-based Electro-active Paper Sensor," Int. J. Precis. Eng. Manuf., Vol. 11, No. 6, pp. 823-827, 2010.
12. Ayers, J. P., Greve, D. W., and Oppenheim, I. J., "Energy Scavenging for Sensor Applications Using Structural Strains," Proc. of Energy Scavenging for Sensor Applications Using Structural Strains, Vol. 5057, pp. 364-375, 2003.
13. Kim, M., Hoegen, M., Dugundji, J., and Wardle, B. L., "Modeling and Experimental Verification of Proof Mass Effects on Vibration Energy Harvester Performance," Smart Materials and Structures,

Vol. 19, No. 4, pp. 45023-45043, 2010.

14. Dayou, J. and Chow, M. S., "Performance Study of Piezoelectric Energy Harvesting to Flash a LED," International Journal of Renewable Energy Research, Vol. 1, No. 4, pp. 323-332, 2011.

15. Dayou, J., Chow, M. S., and Liew, W. H. Y., "Harvesting Electrical Charge from Ambient Vibration Using Piezoelectric Materials," Borneo Science, Vol. 29, No. 3, pp. 23-31, 2011.

16. Chow, M. S. and Dayou, J., "Optimization of Piezoelectric Energy Harvesting System Using Split-width Method," Proc. of 3rd CUTSE International Conference, pp. 154-157, 2011.

17. Sobocinski, M., Leinonen, M., Juuti, J., and Jantunen, H., "Monomorph Piezoelectric Wideband Energy Harvester Integrated into LTCC," Journal of the European Ceramic Society, Vol. 31, No. 5, pp. 789-794, 2011.